THE EFFECT OF TRIAZOLE THIONE DERIVATIVE ON THE CORROSION OF IRON IN HYDROCHLORIC ACID SOLUTIONS

E. M. ATTIA and F. H. ABD EL- SALAM

Chemistry Department, Faculty of Science (for Girls), AL- Azhar University, Cairo, Egypt

Abstract

Surfactant; N-(sodium-2–hydroxy-3-sulphato propyl)-5-stearyl-1,3,4-triazole-2-thione (18PTT) was tested as a corrosion inhibitor for iron electrode in hydrochloric acid media using potentiodynamic polarization measurements. Results obtained show that the corrosion rate (C_R) increases with increasing of free acid concentration. In the presence of the inhibitor, the magnitude of C_R is suppressed as its tendency to increase with acid concentration. The changes in the electrochemical parameters with concentration of surfactant studied are indicative of the adsorption of surfactant leading to the formation of a protective layer on the surface of iron. The inhibition efficiency (IE %) increases with an increase in concentration of surfactant and hydrochloric acid but decreases with temperature. This surfactant suppressed both cathodic and anodic processes of iron corrosion in HC1 solution by adsorption on iron surface according to Langmuir adsorption isotherm but affecting more the anodic reaction than the cathodic one. Thus, it can be classified as mixed-type inhibitor. The thermodynamic parameters for the dissolution of the metal and for the adsorption of the inhibitor on the metal surface were calculated and discussed. In the range of 20-60 °C corrosion rates were found to increase with increasing temperature for inhibited and uninhibited acid solutions, while corrosion potential (E_{corr}) was unchanged. The associated apparent activation corrosion energy (E_a) has been determined and found to be higher in presence than in absence of the inhibitor. The calculated thermodynamic parameters ($\Delta G°$), ($\Delta H°$) and ($\Delta S°$) showed that the inhibition process is spontaneous and exothermic in nature.

Introduction

The corrosion inhibition of iron metal and its steel alloys are of tremendous technological importance due to the increased industrial applications of these materials. Many organic compounds, such as quaternary ammonium salts [1-4], acetylenic alcohol, and heterocyclic compounds are widely used as inhibitors in various industries for preventing corrosion [5-12]. Anionic [13], cationic [14-18] and nonionic surfactants [19] are widely used as corrosion inhibitors. The high affinity of surfactant molecules to adsorb onto interfaces is responsible for their applications in several interfacial systems. For this reason, surfactant; can be used as good corrosion inhibitors for metals [12, 20]. Hetero atoms such as nitrogen, oxygen, sulphur and phosphor atoms, by which the inhibitor molecules are adsorbed on the metal surface in acidic media , thus resulting adsorption film acts as a barrier separating the metal from the corrosive medium and blocks the active sites of metal dissolution and/or hydrogen evolution, thus diminishing the overall corrosion rate [10,21,22]. Heterocyclic substances containing nitrogen atoms, such as triazole-type compounds are

considered to be excellent corrosion inhibitors for many metals and alloys in various aggressive media [8, 16].

The aim of this study is to determine the inhibition efficiency of a new type of triazole thione derivative as an inhibitor for the corrosion of iron in HCl solutions

Experimental

The hydrochloric acid solutions (0.1, 0.3, 0.5, 0.8 and 1.0M) were prepared at room temperature (35°C) using reagent grade concentrated acid and bi-distilled water. The molecular structure of the inhibitor (18PTT) namely N-(sodium-2–hydroxy-3-sulphato propyl)-5-stearyl-1,3,4-triazole-2-thione [23] is represented in Figure (1). The effect of inhibitor concentration (10^{-2} to10^{-6} M) on its inhibition efficiency was examined in 1M HCl at 35°C. The effect of temperature on the inhibition efficiency of 4mmol inhibitor in 0.1M HCl was determined at the range of 20 to 60 °C using potentiodynamic polarization curves.

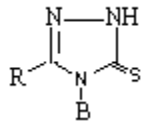

$R= CH_3 (CH_2)_{17}$

$B= CH_2 CHOH CH_2SO_3^-$

Figure (1): Schematic representation of surfactant (18PTT).

The specimen is made of massive cylindrical iron rod (99.99% purity, Alfa Ventron) mounted into glass tube by epoxy resin. A copper wire was employed for electrical contact. The surface preparation of the specimen was carried out using emery paper up to 1200 grade. After polishing, the specimen was washed with distilled water, degreased with acetone and rinsed with bi-distilled water. A cylindrical surface area of 1.643cm^2 was left of the electrode to contact the electrolyte.

Electrochemical experiments were carried out in a double- walled glass cell. Platinum sheet (4cm^2) was used as a counter, while saturated calomel electrode (SCE) provided with a Luggin capillary probe was used as a reference electrode. The corrosion cell was filled with a known amount (30 ml) of test solution. In Tafel plot technique, the anodic E/Log I curves for all solutions were swept from negative to positive potential at scan rate of 10 mV/sec.. Potentiodynamic polarization

measurements were generated using a Wenking Electronic Potentioscan (mode l73). The results are quite reproducible and the indicated results are the mean of four experiments.

Results And Discussion

I- Concentration Effect:

i- Effect of free HCI concentration on corrosion of iron metal

The corrosion behavior of iron metal in different concentrations of HCl at 35°C revealed that when the electrode potential was made to change towards more positive values, the initially high cathodic current density decreased continually and changed its direction at which the rate of cathodic reaction was equal to the rate of anodic one (Figure 2). By further increase of the potential, an active dissolution region was observed where the potential- current relations were linear with the well Tafel slope. The values of E_{corr} and I_{corr} were determined from the extrapolation of cathodic and anodic Tafel lines. The corrosion rate (C_R) of iron metal was calculated using the following equation [24]:

$$C_R = 0.13 \times I_{corr} \times Eq.Wt./d \quad \ldots\ldots (1)$$

Where I_{oorr}, is the corrosion current density in mA/cm^2 and d, is its density in g/cm^3.

When iron corrodes in acid solutions at low pH, the corrosion rate is the same as the rate of anodic iron dissolution.

$$Fe = Fe^{+2} + 2e^- \quad \ldots\ldots (2)$$

And is also the same as the rate of cathodic hydrogen evolution.

$$2H^+ + 2e^- = H_2 \quad \ldots\ldots (3)$$

The reverse reactions of the last two equations (2) or (3) occur at an insignificant rate at low pH. The rate of reaction (2), expressed as current I at potential Є, is known to follow the Tafel equation [25]:

$$Є - Є^{‡} = b_a \text{ Log } (I/I^{‡}) \text{ Or } I/I^{‡} = \exp [(2.303/ b_a) (Є - Є^{‡})] \ldots\ldots (4)$$

Where $Є^{‡}$, is a reference potential.

A similar relation may be written for reaction (3), which is also known to follow the Tafel equation. The obtained results revealed that the corrosion rate increases with

increasing acid concentration (Table 1). This indicates that the aggressive Cl^- ions participate in the dissolution process.

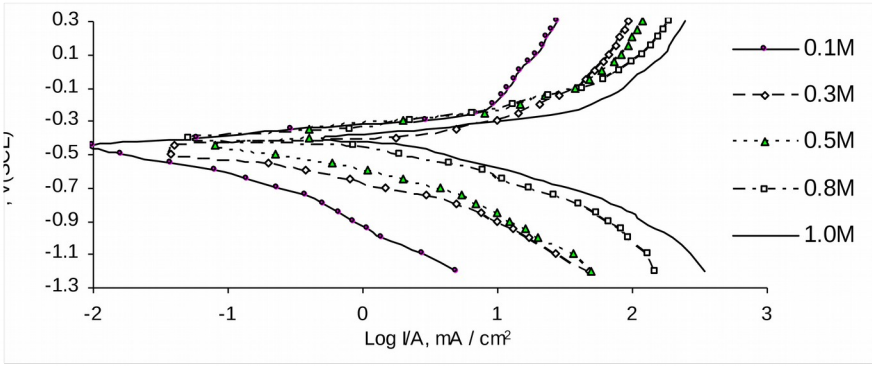

Figure (2): E- Log I curves of iron electrode in different concentrations of HCl solutions.

Table (1): Electrochemical parameters of Fe electrode in different concentrations of HCl at 35°C.

Conc. M	E_{corr} (mV/SCE)	I_{corr} (mA/cm^2)	b_a (mV/dec.)	$-b_c$ (mV/ dec.)	C_R mmpy
0.1	-500	2.8	1005	392	1.54
0.3	-512	12.0	1055	440	6.73
0.5	-400	21.0	901	499	7.85
0.8	-410	39.0	689	952	21.89
1.0	-422	57.0	516	823	23.29

E_{corr}, corrosion potential — I_{corr}, corrosion current density
b_a, b_c anodic and cathodic Tafel slope — C_R corrosion rate

ii- Effect of 18PTT concentration on the corrosion of iron metal

Addition of 18PTT to 1M HC1 at 35°C at different concentrations shifted the corrosion potential in the positive direction by only about 50 mV(SCE). In all concentrations, E_{oorr} was unchanged and has the value of ~ - 350 mV(SCE) (Figure 3 and Table 2).

Increasing of additive concentration up to 10^{-2} M lowered corrosion current densities. This can be correlated with the increasing degree of surface coverage (Θ) due to adsorption of the additive on the iron surface as the inhibitor concentration was increased [26]. In cathodic region, curves of concentrations range from 10^{-6} to 10^{-3} are nearly coinciding with the curve of free HC1 solution, while 10^{-2} M surfactant

shifts the current density to lower values. In anodic region, 18PTT shifts the potential towards more noble values with increasing concentration, indicating the inhibition effect of this compound on the corrosion of iron metal in 1M HCl affecting more the anodic reaction than the cathodic[27].

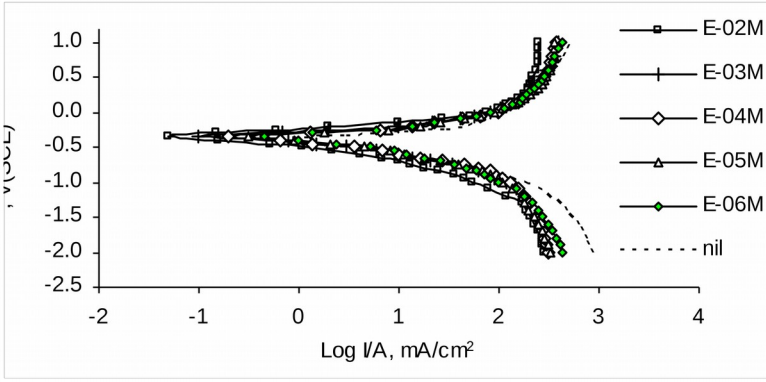

Figure (3): E – Log I curves of iron electrode in 1M HCl containing different concentrations of 18PTT.

Table (2): Electrochemical parameters of Fe electrode in 1M HCl containing different concentrations of 18PTT at 35 °C.

Conc. M	E_{corr} (mV/SCE)	I_{corr} (mA/cm^2)	b_a (mV/dec.)	$-b_c$ (mV/dec.)	C_R mmpy	IE %
nil	-400	41.5	227	217	23.29	–
E-06	-353	37.5	312	333	21.05	09.6
E-05	-351	33.0	333	278	18.52	20.5
E-04	-350	32.5	322	231	18.24	21.7
E-03	-350	27.5	278	283	15.43	33.7
E-02	-347	11.5	227	370	06.45	72.3

E_{cor}, corrosion potential I_{cor}, corrosion current density
b_a, b_c anodic and cathodic Tafel slope C_R corrosion rate

Experimental determination of the cathodic Tafel slope for iron metal in different concentrations of surfactant solution gave values closed to b_c = -2.303 RT/0.22F, which is in accord with (but does not itself establish) a slow H^+ discharge mechanism for the hydrogen evolution reaction [28]. An experimental determination of b_a, however, has not varied significantly. It gave b_a values closed to 2.303RT/0.21F. This value is not identical with the theoretical Heusler[29] and Bockris *et a*/.[30] mechanisms (b_a = 2.303 RT/2F and 2.303 RT/1.5F respectively).

The inhibition efficiency, IE %, was calculated from the following equation [31]:

$$IE\ \% = \left[1 - \frac{I_{corr}}{I^{o}_{corr}}\right] x\ 100 \quad \ldots\ldots\ldots\ldots\ldots\ldots (5)$$

where I^{o}_{corr} and I_{corr} are the corrosion current densities obtained in uninhibited and inhibited solutions. It can be found that, the inhibition efficiency increases with an increase in additive concentration.

Adsorption isotherms

Inhibitors can function by physical adsorption, chemisorptions or by complexation with the metal. Attempts were made to fit Θ values to kinetic thermodynamic model (Eq.6)[32, 33]

$$\text{Log } (\Theta /1- \Theta) = \text{Log } k` + y \text{ Log } C_{inh} \quad \ldots\ldots\ldots\ldots\ldots\ldots (6)$$

where Θ is a degree of coverage (Θ = IE %/100 [34]), y is the number of inhibitor species occupying one active site, C_{inh} is the inhibitor concentration in the bulk of solution, and k' is related to the equilibrium constant by:

$k^{`\left[\frac{1}{y}\right]} = K$ where K is the binding constant (equilibrium constant of the adsorption reaction). A plot of Log (Θ/I - Θ) against Log C_{inh} for different concentrations is shown in Figure (4).

Langmuir adsorption isotherm is generally regarded to indicate adsorption of inhibitors on the metal. This is achieved by plotting (Log Θ)/(l- Θ) against Log C_{inh}, where C_{inh}, is the molar concentration of the inhibitor[35]. A straight line relationship with a slope of 0.1385 was observed (Figure 4). Another form of the Langmuir model as reported by Eligwe *et al*. is [36]:

$$C_{inh}/ \Theta = 1/KBs + C_{inh} /B_s \quad \ldots\ldots\ldots\ldots\ldots\ldots\ldots (7)$$

where C_{inh}, is the molar inhibitor concentration, Θ, is the surface coverage, B_s, is the sorbent binding capacity, that is, the maximum sorption upon complete saturation of adsorbent surface and K, is the binding constant, that is, related to the adsorption/ desorption energy and is defined as [21]

$$K = \frac{1}{C_{solvent}} \exp\left(\frac{-\Delta G_{ads}}{RT}\right) \quad (8) \ldots\ldots\ldots$$

Where $C_{solvent}$, is the molar concentration of the solvent, which in case of water is 55.5 mol L^{-1}. R, is the universal gas constant, 8.314 J/mol K, T is the absolute temperature and ΔG_{ads}, is the adsorption free energy.

Plots of C_{inh}/Θ versus surfactant concentration could be obtained (Figure 5). Comparing the values of linear correlation coefficient, R^2, for the two Langmuir models illustrate that the latter model fit the experimental results better than the former.

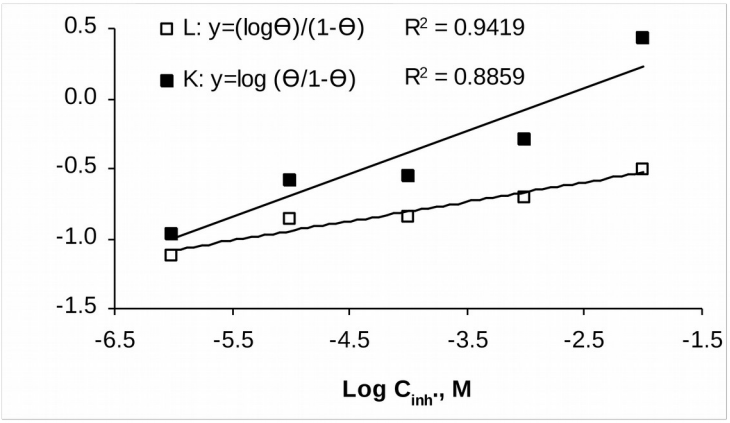

(L) represents Langmuir adsorption isotherm and (K) represents Kinetic - Thermodynamic adsorption isotherm.

Figure (4): Representation of Langmuir and Kinetic- Thermodynamic adsorption isotherms of 18PTT on the iron surface.

The linear correlation coefficient (R^2) and the adsorption parameters for the kinetic thermodynamic and the second Langmuir model of the adsorption of 18PTT onto iron surface at 35°C were calculated and the results are shown in Table (3). It was observed that the value of binding constant, K as obtained from the kinetic-thermodynamic model is low compared with that obtained from Langmuir isotherm. The value of 1/y indicating that 18PTT molecule is mainly adsorbed at three active sites of the metallic surface at 35°C [37]. On the other hand, the correlation coefficient for Langmuir's adsorption isothermal equation approaches 1.0 which illustrates that the adsorption of the surfactant on the iron surface conforms to this model.

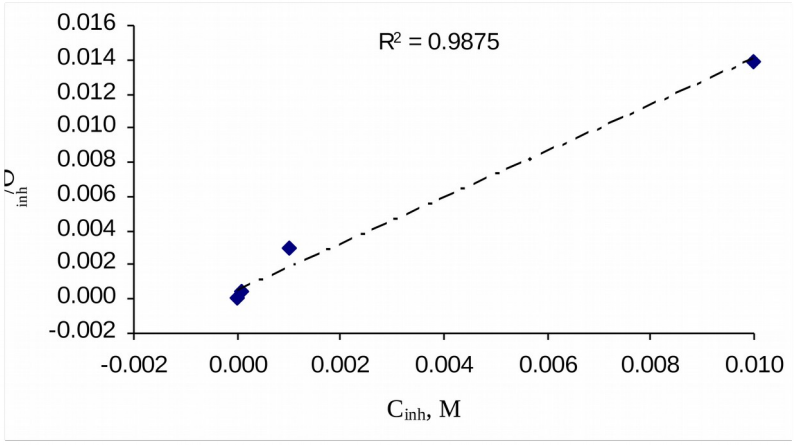

Figure 5: Dependence of C_{inh}/θ on the concentration of 18 PTT in 1MHCl at 35 °C.

Table 3: Adsorption parameters of 18 PTT on the iron surface in 1M HCl at 35 °C

Kinetic - thermodynamic		Langmuir	
R^2	0.88	R^2	0.98
K	498	K	2695
y	0.31	B_S	0.74
1/ y	3.25	ΔG_{ads} kJmol^{-1}	-31

The negative value of ΔG_{ads} indicates that the adsorption reaction is proceeding spontaneously [38].This isotherm gave a very good description of the sorption process over the range of concentration studied.

When 18PTT is dissolved in acid, protonation occurs. Adsorption of Cl^- ions may act to displace the potential of zero charge to a value more positive than the observed E_{corr} for iron in 1M HC1 (-400 to -350 mV(SCE)). This would make the iron negatively charged and susceptible to physical adsorption of the positively charged inhibitor species [39]. The long chain surfactant compound reduced the number of active sites on the surface of iron and hence facilitated its corrosion inhibition [40].

iii- Effect of HC1 concentration on the inhibition efficiency of 18PTT on the corrosion of iron

The effect of changing HCl concentration on the inhibition efficiency of 18PTT was investigated. The current responses in Figure (6) are typical for polarization runs in the solutions containing 4mmol 18PTT with various acid concentrations. It is obvious that increasing acid concentration resulted in increasing IE % up to a maximum of approximately 0.8M HCl (Figure 7). The maximum inhibition efficiency of 18PTT was approximately 59 %.

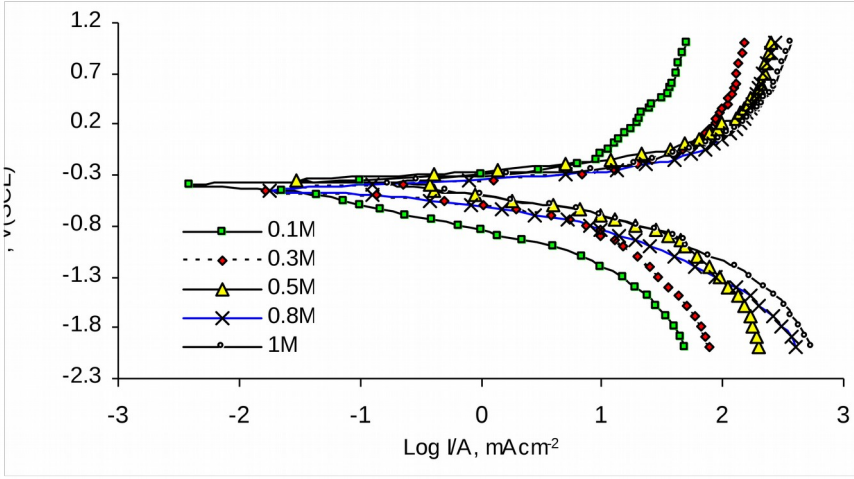

Figure (6): Potentiodynamic polarization curves of Fe electrode in 4mmol 18PTT soluble in different concentrations of HCl solutions.

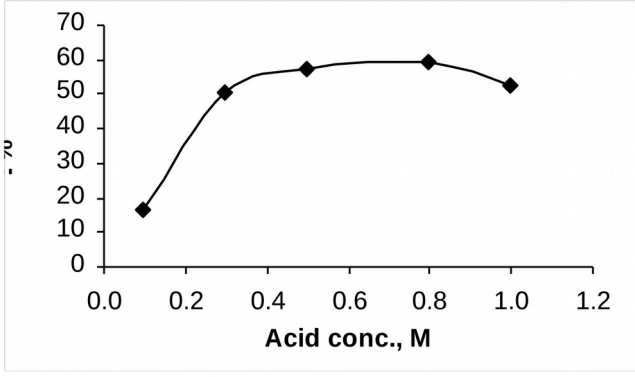

Figure (7): Effect of HCl concentration on IE% at 4mmol level of 18 PTT for iron electrode.

The natural logarithm of the corrosion rate (C_R) of 18PTT versus the molar concentration of HCI obtained a straight line relationship whose slope decreased at

approx. 0.3 M HCl for the blank and surfactant solution. The following rate equation was set up [41] to describe the straight line relationship.

$$\ln C_R = \ln k + BC \quad \text{.....(9)}$$

Where k is the specific reaction rate constant, B is a constant for a reaction and C is the molar concentration of the acid. Equation (9) is shown graphically in Figure (8) and calculated kinetic parameters are listed in Table (4). In the presence of inhibitor, the magnitude of C_R is suppressed as its tendency to increase with acid concentration. This may be due to suppression of iron chloride by the adsorption of the surfactant. The decrease of slope of the blank and inhibited solution may be arise from the formation of a tightly adsorbed, more protective iron chloride compound on the metal at higher acid concentrations (> 0.3M). This behavior is similar to low carbon steel in phosphoric acid solution [39].

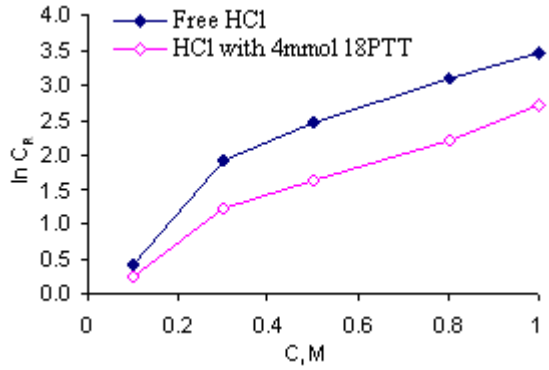

Figure (8): Variation of $\ln C_R$ with concentration of HCl in presence and absence of 4mmol 18PTT for iron metal at 35°C.

Table (4): Calculated values of kinetic parameters for the corrosion of iron in HCl solutions in presence and absence of 18 PTT

Medium	B mg $m^{-2}s^{-1}M^{-1}$		K mg $m^{-2}s^{-1}$	
Free HCl	B_1	7.4	K_1	0.74
	B_2	2.2	K_2	3.67
HCl solutions containing 4mmol 18PTT	B_1	4.8	K_1	0.79
	B_2	1.9	K_2	1.88

Subscript 1 refers to concentration range from 0.1 to 0.3M;
Subscript 2 refers to concentration range from 0.3 to 1M

II- Temperature Effect on corrosion of Fe Electrode

i- Effect of temperature of 0.1 M HCl on corrosion of Fe electrode

Clearly the increase in solution temperature increases the current density at a certain potential and correspondingly increases the corrosion rates, while E_{corr} was unchanged (Figure 9 and Table 5). It was suggested that the critical factor in corrosion process is the rate at which a metal surface repassivates after the original passive film has been ruptured by slip- step emergence, etc[25]. Therefore, at higher temperatures, metals in the potential regions near the active- passive [42] where the surface is still filmed but the impetus for passive film renewal is somewhat slow should be more susceptible to corrosion.

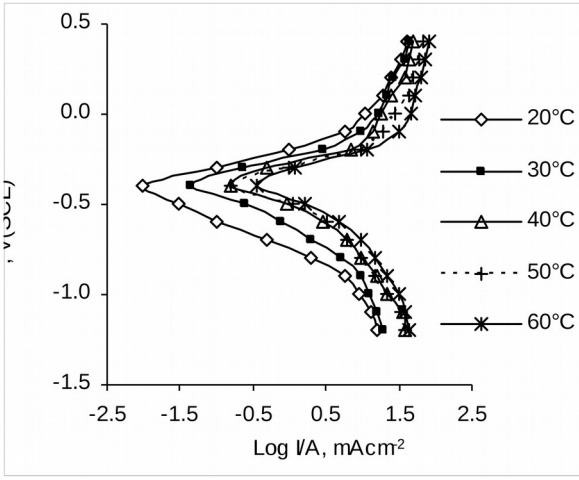

Figure (9): E- Log I curves of iron electrode at different temperatures of 0.1MHC1 solution.

Table (5): Electrochemical parameters of Fe electrode at different temperatures of 0.1M HCl solutions

T °C	E_{corr} (mV/SCE)	I_{corr} (mA/cm^2)	b_a (mV/dec.)	$-b_c$ (mV/dec.)	C_R mmpy
20	-400	06.0	823	704	03.4
30	-400	07.5	996	968	04.2
40	-400	09.0	693	568	05.1
50	-400	12.0	161	565	06.7
60	-400	18.5	1500	1351	10.4

E_{corr}, corrosion potential I_{corr}, corrosion current density

b_a, b_c anodic and cathodic Tafel slopes C_R corrosion rate

ii- Effect of temperature on the corrosion of iron in presence of 18PTT

The data of Tables (5 and 6) with the behaviors given in Figures (9 and 10) show that corrosion rates were found to increase with the increase in temperature for

inhibited and uninhibited acid solutions. The inhibition efficiency of 18PTT at different temperatures decreases with increasing temperature, suggesting that physical adsorption may be the type of adsorption of the surfactant on the iron surface[43]. Surfactant effect appears to be dependent on the temperature of the medium. This may be attributed to desorption of the inhibitor molecules from the metal surface at elevated temperatures leading to a greater area of metal being exposed to corrosive medium [43].

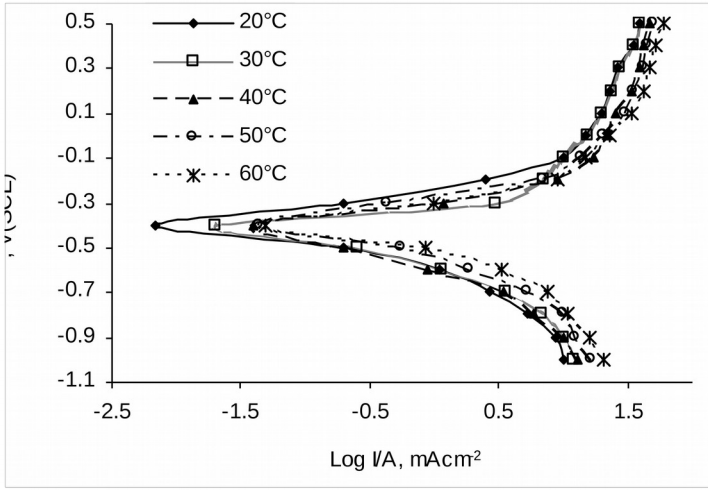

Figure (10): E- Log I curves of iron electrode in 0.1M HCl containing 4mmol 18PTT at different temperatures.

Table (6): Electrochemical parameters and the corresponding inhibition efficiency of iron electrode in 4mmol 18PTT soluble in 0.1M HC1 at different temperatures

T °C	E_{corr} (mV/SCE)	I_{corr} (mA/cm^2)	b_a (mV/dec.)	$-b_c$ (mV/dec.)	C_R mmpy	I E %
20	-400	3.50	664	1786	1.96	56.25
30	-433	3.70	580	1266	2.08	50.67
40	-450	4.70	196	909	2.64	47.78
50	-467	7.10	580	870	3.98	40.83
60	-475	12.0	563	712	6.73	35.13

E_{corr}, corrosion potential — I_{corr}, corrosion current density
b_a, b_c anodic and cathodic Tafel slopes — C_R corrosion rate

The activation parameters are obtained from an Arrhenius-type plot (Eq. 10) [33] and Eyring transition-state (Eq. 11)[44].

$$\text{Log } C_R = A - (E_a / 2.303\ RT) \quad \ldots\ldots\ldots\ldots\ldots\ldots\ldots\ldots\ldots\ldots\ldots \quad (10)$$

$$\text{Log } C_R/T = \text{Log } R/Nh + \Delta S°/ 2.303\ R - (\Delta H°/2.303RT) \ldots\ldots\ldots \quad (11)$$

Where E_a is the apparent activation energy, R is the ideal gas constant, h is Planck's constant, ΔS° is the entropy of activation, N is Avogadro's number, ΔH° is the enthalpy of activation and T is the absolute temperature.

Plots of Log C_R against 1/T (Figure 11) and Log (C_R /T) against 1/T (Figure 12) gave straight lines with slops of (E_a/2.303R) and (ΔH° /R), respectively. The calculated values of E_a, **Δ**H° and **Δ**S° obtained from these plots are tabulated in Table (7). The data clearly show higher value of E_a in the inhibited solution than that in the uninhibited one.

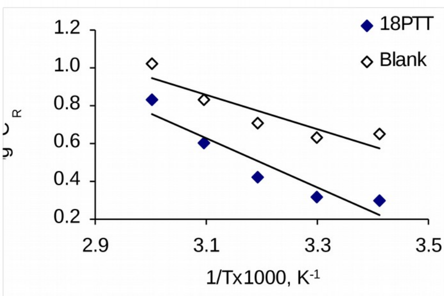

Figure11: Arrhenius plot of the corrosion rate of iron in 0.1 M HCl in the absence and presence of 4mmol 18PTT.

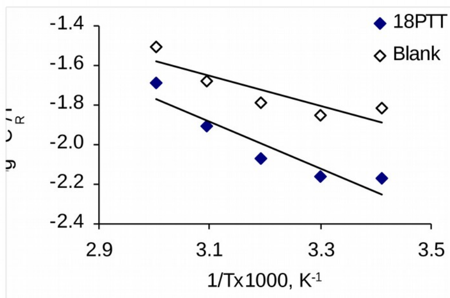

Figure 12: Transition-state plots of the corrosion rate of iron in 0.1 M HCl in the absence and presence of 4mmol 18PTT.

Table (7): The values of activation parameters for iron in 0.1M HC1 in the absence and presence of 18PTT

Medium	E_a ($kJmol^{-1}$)	ΔH° ($kJmol^{-1}$)	ΔS° ($JK^{-1}\ mol^{-1}$)
Blank	17.11	14.52	-184.20
18PTT	24.97	22.37	-164.29

The higher activation energy values explain the corrosion inhibition obtained [(26)]. The above table also shows that the presence of the inhibitor produces higher values for ΔH° than those obtained for the uninhibited solution indicating higher protection

efficiency. This may be attributed to the presence of an energy barrier for the reaction, that is, the process of adsorption leads to a rise in the enthalpy of the corrosion process [45]. The table illustrates also that ΔS° has negative value for the blank and 18PTT solutions. This may be discussed as follows, in the blank solution; the transition state of the rate determining recombination step represents a more orderly arrangement. Hence, a negative value for the entropy of activation is obtained. In the presence of the 18PTT, however, the rate-determining step is the discharge of hydrogen ions to form adsorbed hydrogen atoms. Since the surface is covered with the surfactant molecules, this will retard the discharge of hydrogen ions at the metal surface causing the system to pass from a more to a less orderly arrangement. This was unlike to the results of Grigorev and co-workers [46, 47] and Antropov and Suvgira [48] in which ΔS° has negative value for the test solution and turned positive in the presence of surfactant which means that his system passes from a more orderly to a random arrangement.

Conclusion

The corrosion rates of iron metal increase with increasing free acid concentration and decrease with the increase of surfactant (18PTT) concentration. 18PTT inhibits the corrosion of iron in 1M HC1 affecting more the anodic reaction than the cathodic one and acts as mixed type inhibitor. Increasing acid concentration on 4mmol surfactant resulted in increasing IE % for iron metal. The adsorption process of inhibitor follows Langmuir model and the reaction is proceeding spontaneously. Corrosion rates were found to increase with the increase in temperature for inhibited and uninhibited acid solutions. The inhibition efficiency of 18PTT at different temperatures decreases with increasing temperature. E_a, ΔH°, ΔS°, indicates the corrosion inhibition obtained higher protection efficiency.

References

1. M.M. OSMAN, A.M.A. OMAR, A.M. AL-SABAGH; Mater. Chem. Phys. 50 (1997) 71.

2. M.M. SALEH, A.A. ATIA; J. Appl. Electrochem. 36 (2006) 899.

3. L. NIU, H. ZHANG, F. WEI, S. WU, X. CAO, P. LIU; Appl. Surf. Sci. 252 (2005) 1634.

4. S. MOHANAN, S. MARUTHAMUTHU, N. KALAISELVI, R. PALANIAPPAN, G. VENKATACHARI, N. PALANISWAMY, M. RAGHAVAN; Corros. Rev. 23 (2005)

425.

5. M.L. FREE; Corros. Sci. 44 (2002) 2865.

6. M.A. MIGAHED, H.M. MOHAMED, A. M. AL-SABAGH; Mater. Chem. Phys. 80 (2003) 169.

7. M.A. QURAISHI, H.K. SHARMA; Mater. Chem. Phys. 78 (2002) 18.

8. D. CHEBABE, Z.A. CHIKH, N. HAJJAJI, A.A. SRHIRI, F. ZUCCHI; Corros. Sci. 45 (2003) 309.

9. F. BENTISS, M. TRAISNEL, L. GENGEMBRE, M. LAGREN'EE; Appl. Surf. Sci. 161 (2000) 194.

10. F. BENTISS, M. LAGREN'EE, M. TRAISNEL, J.C. HORNEZ; Corros. Sci. 41 (1999) 789.

11. V. O. ALEGO, N. HUYNH, T. NOTOYA, S.E. BOTTLE, D.P. SCHWEINSBERG; Corros. Sci. 41 (1999) 685.

12. E. F. MOURA, A. O. W. NETO, T. N. C. DANTAS, H. S. JÚNIOR, A. GURGEL; Collo. Surf. A: Physicochem. Eng. Asp. 340 (2009) 199.

13. M.A. DEYAB, S.S. ABD EL-REHIM, S.T. KEERA; Collo. Surf. A: Physicochem. Eng. Asp. 348(2009) 170.

14. L. HUANG, C. MALTESH, P. SOMASUNDARAN; J. Collo. Interf. Sci. 177 (1996)222.

15. J. SAVKOVIC-STEVANOVIC, T. MOŠORINAC, B. R. SNEŽANA, D. B. RUŽICA; Computer Aided Chem. Eng. 24 (2007)195.

16. L-G QIU, A-J XIE, Y-H SHEN; Mater. Chem. Phys .91 (2005) 269.

17. G. LISSENS, J. PIETERS, M. VERHAEGE, L. PINOY, W. VERSTRAETE; Electrochim. Acta 48(2003)1655.

18. Y. KUWAHARA, A. GOTO, Y. IBUKI, K. YAMAZAKI, R. GOTO; J. Collo. interf. Sci. 233 (2001)190.

19. X. LI, S. DENG, G.MU, H. FU, F. YANG; Corros. Sci. 50(2008) 420.

20. R. VITTAL, H. GOMATHI, K-J KIM; A. Collo. Interf. Sci. 119(2006)55.

21. L-G QIU, Y. WU, Y-M WANG, X. JIANG; Corros. Sci. 50 (2008)576.

22. B. MERNARI, H. ELATTARI, M. TRAISNEL, F. BENTISS, M. LAGRENEE; Corros. Sci. 40 (1998)391.

23. Unpublished data, Assistant Professor Dr. F. H. ABD EL- SALAM; Applied organic chemistry, Faculty of Science (Girls), Al-Azhar University. Cairo, Egypt.

24. V. BRANZOI, F. BRANZOI, M. BAIBARAC; Mater. Chem. Phys. 65 (2000) 288.

25. S. BARNARTT; J. Electrochem. Soc. 119(1972) 812

26. G. QUARTARONE, L. BONALDO, C. TORTATO; Appl. Surf. Sci. 252 (2006) 8251.

27. H. VAIDYANATHAN, H. HACKERMANN; Corros. Sci. 11(1971)737.

28. J. J. BOCKNS, D. DRAZIC, A. R. DCIPIC; Electrochim. Acta 4 (1961) 325.

29. K. E. HEUSLER, G. H. CARTLEDG; J. Electrochem. Soc. 108(1961) 732.

30. J.M. BOCKRIS, D. DRAZIC; Electrochim. Acta 7 (1962) 293.

31. R.A. PRABHU, T.V. VENKATESHA, A.V. SHANBHAG, G.M. KULKARNI, R.G. KALKHAMBKAR; Corros. Sci. 50 (2008) 3356

32. A. EL-AWADY, B. ABD EL- NABEY, G. AZIZ; J. Electrochem. Soc. 139 (1992)2149.

33. M. A. DEYAB; Corros. Sci. 49 (2007)2315.

34. G. MORETTI, G. QUARTARONE, A. TASSAN, A. ZINGALES; Werkst Korros. 45 (1994) 641.

35. E. M. ATTIA; Al- Azhar Bull. Sci.19 (2008)135.

36. C.A. ELIGWE, C.I.A. NWOKO, U.U. EGERREONU; J. Chem. Soc. of Nigeria. 24(1999)70.

37. A. EL-AWADY, B.ABD EL-NABEY, G.AZIZ, M. KHALIFA, H. AL-GHAMDY; Int. J. Chem. 1(1991) 169.

38. J.D. TALATI, D.K. GANDHI; Corros. Sci. 23 (1983) 1315.

39. Y. JIANGUO, W. LIN, V. OTIENO-ALEGO, D. P. SCHWEINSBERG; Corros. Sci. 37(1995)975.

40. K-C TSAI, N. HACKERMAN; J. Electrochem. Soc. 118(1971)28.

41. P.B. MATHUR, T. VASUDEVAN; Corros. 38(1982) 171.

42. R. N. PARKINS; Br. Corros. J. 7 (1972) 15.

43. E.E. FOAD EL-SHERBINI, S.M. ABD EL WAHAB, M.A. DEYAB; Mater. Chem. Phys. 82 (2003) 631.

44. S. S. ABD EL REHIM, H. H. HASSAN, M. A. AMIN; Mater. Chem. Phys. 70 (2001) 64.

45. M.A. AMEER, E. KHAMIS, G. AL-SENANI; J. Appl. Electrochem. 32 (2002) 149.

46. V.P. GRIGOREV, V.U. EKLIK; Prot Met. 4(1968) 517.

47. V.P. GRIGOREV, O.A. OSIPOV; in: 3rd European Symposium on Corrosion Inhibitors, Ferrara, Italy. 1970, p. 473.

48. L.A. ANTROPOV, Y.A. SUVGIRA; Prot. Met. 3 (1967) 597.